Ultrasonic Range Finder

ENG PHYS 3BA4
William Ward
400170514

Fall 2021

1 Executive Summary

This projected consisted of a team of Engineering Physics students that built an Ultrasonic Ranger Finder using fundamental electronic components. The purpose of the device was to provide a digital readout of the distance to an object within a range of $10-99\ cm$ with an accuracy of $\pm 1\ cm$ using ultrasonic acoustic waves. Analog and digital electronic components were consolidated into a single working prototype in order to achieve this goal. The accuracy of the final device was found to $\pm 2\ cm$ over the required working range of the device. This project demonstrated that fundamental electronic components, each with a specific function, can be combined to create a functional device when designed properly.

2 Introduction

The objective of the Ultrasonic Range Finder design project is to provide a digital readout of the distance to an object from the sensing device using ultrasonic sound waves. The design project is meant to encourage students to utilize and combine their knowledge of analog & digital electronics to work towards a goal. This project is important because it requires the synthesis of independently learned knowledge to solve a specific problem. This type of synthesis is a more realistic application of electronics with regards to solving a problem. Since this project spans multiple weeks, it also provides students with the opportunity to learn about time management, top-down design, bottom-up synthesis and improve their general problem solving skills. The Ultrasonic Ranger Finder device will utilize acoustic waves in order to measure a distance.

2.1 Device Overview and Functional Description

In this section, a high-level overview is presented which includes a general description of each module utilized by the device. A detailed block diagram is included in section (4). More detailed explanations of each module are included in the Methods section (4). As mentioned previously, the device will utilize ultrasonic sound waves in order to determine the distance to an object from the device.

2.1.1 Wave Packet Generation

In order to drive the piezoelectric transducer in the most efficient manner possible, a 40 kHz voltage signal needs to be fed to the transducer [4]. However, constantly driving the transducer with a 40 kHz signal would render determining the time-of-flight of the sound wave very difficult. Thus, it was decided that the transducer driving signal must be modulated by a lower frequency signal. In order to achieve this result, two 555 timers were utilized. Both 555 timers were used as astable multivibrators (see figure (2) in section (4)). The astable multivibrators were used to create a 40 kHz driving signal, and a lower frequency modulating signal, respectively. These signals were combined to create a wave packet using appropriate digital components.

2.1.2 Pre-Amplification, Post-Amplification & Digitization

Amplification of the transmitted and received signal was necessary for multiple reasons. The received signal was small in magnitude at farther detection distances, thus two amplification stages were necessary in order to amplify the signal to an appropriate amplitude. Two filters were necessary before each post-amplification stage in order to avoid amplifying noise. The post-amplification module ensures that the received signal amplitude is appropriate for conversion into a digital signal. the pre-amplification stage was put in place to increase the amplitude of the received signal at a given reflection distance. The purpose of this module is to decrease the magnitude of the post-amplification gain stage, and increase the signal-to-noise ratio of the received signal. Digitization of the amplified receive signal was necessary in order to use the received signal to count during the conversion from TOF (Time of Flight) to distance.

A custom Schmitt trigger was utilized to digitize the signal appropriately.

2.1.3 Counting Wave Packet Generation

As mentioned earlier in the introduction, the *TOF* signal received must be converted into a distance. To realize this goal, the *TOF* pulse was used as a modulating wave for a high frequency square wave. The appropriate square wave frequency was chosen in order to equate each pulse to 1 *cm* that the transmitted sound wave travelled. More specific justification for this choice is presented in section (4.3.2).

2.1.4 Counting and Display

The device utilizes two BCD counters, configured as an asynchronous ripple-counter in order to produce a digital output based on a total pulse count. The counting wave packet was fed into the asynchronous ripple counter configuration. The binary output of the asynchronous ripple counter configuration was decoded and displayed on two seven-segment displays. These displays represent the distance that was determined by the device in centimeters. The 4-bit output of the first counter in the ripple-counter series represents the 4 least significant bits, and the output of the second counter in the ripple-counter series represents the most significant bits of the calculated 8-bit binary number. This is the final module in the device that communicates the distance to the object of interest from the sensor.

3 Theory

The basic operating principle of the Ultrasonic Range Finder depends on the properties of sound in the ultrasound frequency range and the properties of piezoelectric materials. The device works by emitting sounds waves in the ultrasonic frequency range, receiving a the same sound wave after it has been reflected off of the object of interest and determining the time of flight of the sound wave. Once the time of flight is known, the distance to the object of interest can be determined since the speed of sound in the transmission medium is known. The distance can be quantified using the equation(s) below, where d is the distance to the object, and TOF is the time of flight of the sound wave from transmission to reception.

$$v_{sound} = 34300 \ \left[\tfrac{cm}{s}\right]$$
$$d = v_{sound} \times \tfrac{TOF}{2} \, [cm]$$

3.1 Piezoelectric Materials

The most important physical component utilized in this design is the *Air Ultrasonic Ceramic Transducer*[4]. This module includes a piezoelectric material, which has two possible functions. Piezoelectric materials have a property such that when a time-varying voltage is applied across the physical bounds of the material, the crystal structure deforms mechanically. The reverse situation also occurs; when an piezoelectric material is compressed, a voltage is produced due to net charge accumulation as dipoles in the crystal are shifted. Both of these properties of piezoelectric materials are utilized in order to transmit and receive ultrasonic sound waves, respectively.

Piezoelectric materials exhibit these properties because of the atoms that form their crystal structure. When a piezoelectric material is at rest, the positions of the charges due to the atoms within the crystal structure are oriented such that there is no net dipole moment. This implies that at every point in the lattice of a piezoelectric material, the positive and negative charges cancel when no stress is applied to the crystal. For reference, a dipole moment is the product of the separation of two oppositely charges entities by the magnitude of the charges [3]. When a piezoelectric material is stressed by an applied force, many individual dipoles within the material become aligned and an electric field is formed. In this scenario, the charge equilibrium within the crystal structure of the piezoelectric material is disturbed, and net dipole moment is formed. This dipole moment can be represented as a separation of charges;

see figure (1). The separation of charges creates an electric field, which is realized as a voltage across opposite faces of the crystal. When a time-varying voltage is applied to different surfaces of the crystal, the opposite effect is observed. The crystal deforms with the periodicity of the applied voltage due to the force applied on the crystal lattice by the time-varying voltage.

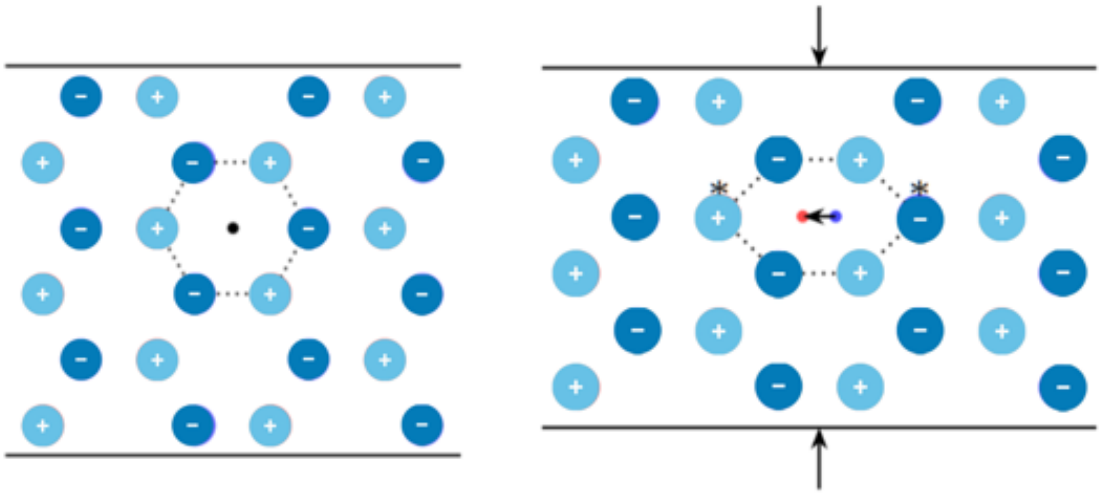

Figure 1: Piezoelectric Crystal Mechanical Deformation [1]

In this design project, piezoelectric materials are extremely useful because the same material functions as both the transmitting and receiving module of the device. In order to create and transmit an ultrasonic sound wave, the *Air Ultrasonic Ceramic Transducer* needs to be driven at 40 kHz [4]. This frequency is the resonant frequency of the particular piezoelectric material utilized in this projects. There are other frequencies at which the piezoelectric material will oscillate when driven by an electric signal (a time-varying voltage). This range of frequencies constitutes the bandwidth of the device [4]. However, the resonant frequency is the point at which the electrical signal is converted into mechanical oscillations most efficiently. Thus, if the device were to be driven at frequencies outside of the operational bandwidth, the pressure waves created by the piezoelectric material would have a relatively low amplitude and quickly attenuate. Driving the device at the resonant frequency ensure pressure waves of maximum amplitude are created, and enables the receiving piezoelectric transducer to detect reflected sound waves at higher reflection distances. When driven at the resonant frequency, mechanical vibrations of the ceramic disc creates pressure waves (sound waves) that propagate outward from the device. The other ceramic disc is constructed in the same fashion, yet it is utilized to receive the reflected sound wave. When the reflected ultrasonic sound wave reaches and interacts with the ceramic disc, the pressure variations propagate through the ceramic disc and create a time-varying voltage across two surfaces of the material. This time-varying voltage is the received signal used to determine the time-of-flight of the sound wave. This is the basic operating principle of the *Air Ultrasonic Ceramic Transducer* that is used to determine the distance to an object by the Ultrasonic Range Finder module.

3.2 Ultrasound

The generally accepted frequencies that fall within the ultrasound range correspond to sound waves with a frequency of $20kHz - 200MHz$ [2]. Sound waves propagate via pressure variations in space and time. Thus, driving one of the ceramic ultrasonic discs at a frequency in the ultrasonic range will produce a pressure wave that propagates through air and corresponds to an ultrasonic sound wave. This propagating wave reflects off of physical barriers. This is the working principle of the range finder; as the transmitted wave is reflected off of a physical barrier, the reflection is then detected by the

receiving ceramic piezoelectric disc. As the reflected wave is incident upon a piezoelectric disc, the pressure variations caused by the wave cause periodic deformation of the material. Since the material is piezoelectric, this periodic deformation produces a voltage that varies at the frequency of the mechanical deformations of the crystal. This voltage is then processed as an electronic signal, and the time of flight if the transmitted ultrasonic sound wave is used to determine the distance that the sound wave traversed. As the speed of sound through air at a given temperature and pressure is known, the time of flight information can be converted into distance information in order t quantity the distance at which the transmitted sound wave reflected off of a physical barrier and was later received by the receiving piezoelectric disk. This is the basic working principle of the ultrasonic range finder.

3.3 Attenuation

When a sound wave propagates through a medium, the amplitude of the wave is decreased; or the wave is *attenuated* for a variety of reasons. When the Ultrasonic Transducer receives the reflected ultrasound signal, the signal has decreased in amplitude when compared to the electrical signal used to produce the pressure waves (note that I use the terms *Pressure Waves* and *Sound Waves* synonymously in this report). Attenuation of the incident and reflected waves mainly occurs due to absorption. When the pressure wave propagates through air, the wave is attenuated when interacting with gas molecules in the air and the energy of the wave is dissipated as thermal energy due to the viscosity of the medium of propagation [5]. Additionally, when the pressure wave is reflected off of the surface of interest, some of the incident wave is absorbed by the molecular structure of the surface, rather than reflected by the surface. There are other second-order effects that contribute to attenuation as well that are not as relevant to this project. Absorption by the propagation medium as well as the object of interest are the main reasons for attenuation of transmitted sound wave. Consequently, the electric signal produced by the receiving end of the ultrasonic transducer is also attenuated. Thus, it must be amplified. Amplifiers are discussed briefly in the next section.

3.4 Signal Processing

An electronic component known as an operational amplifier is required at many stages throughout this project. Thus, it is important to provide a brief background regarding operational amplifiers in order to inform the readers' understanding of the signal processing methods utilized during the construction of the individual modules utilized to construct the device. Operational amplifiers can reliably amplify a small signal. They generally have a high input impedance, and low output impedance. Both of these properties are important as they facilitate maximum voltage transfer when amplifying a signal. In this project, amplifiers are used to ensure the signal is large enough in amplitude to be useful, and maximize the SNR (Signal-to-Noise ratio).

4 Methods

A high-level block diagram that describes the function of the device and integral components is presented below in figure (2). Note that the diagram is separated into a functional hierarchy based on the necessity and contribution of each component. Furthermore, the methods by which the necessary component values were determined is delineated in this section of the report. Each module is described as the sum of different operational units, each of which has a specific purpose. These units, as well as their circuit diagrams are presented in the sub-sections below.

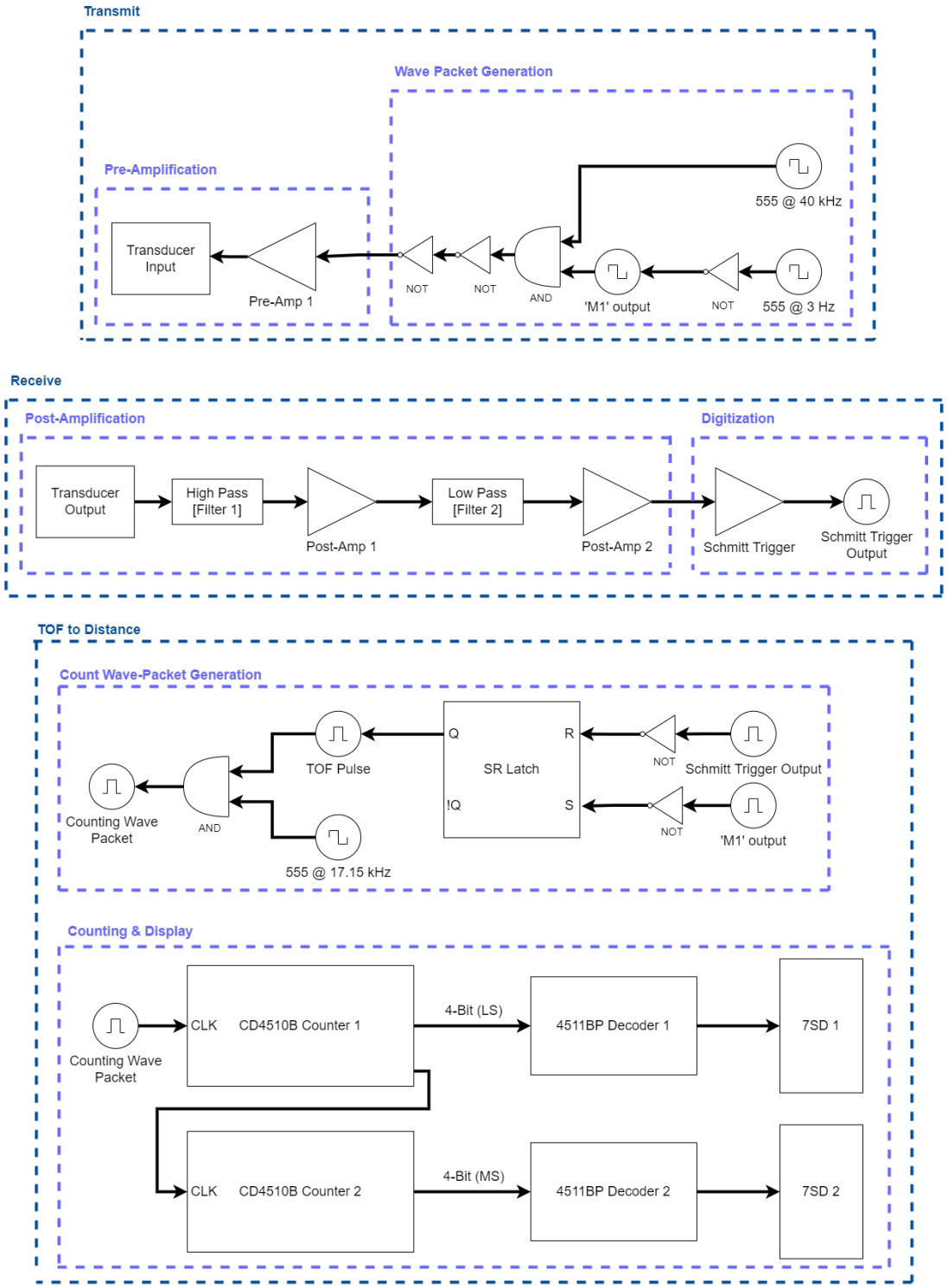

Figure 2: Functional Device Block Diagram

Two timing diagrams the describes the digital processing performed by the device is displayed. Figure (3) demonstrates the case when the object of interest is at the minimum detection distance of $10/cm$. Figure (4) demonstrates the timing of the digital components of the device in the case where the object of interest is at the maximum detection distance of 99 cm.

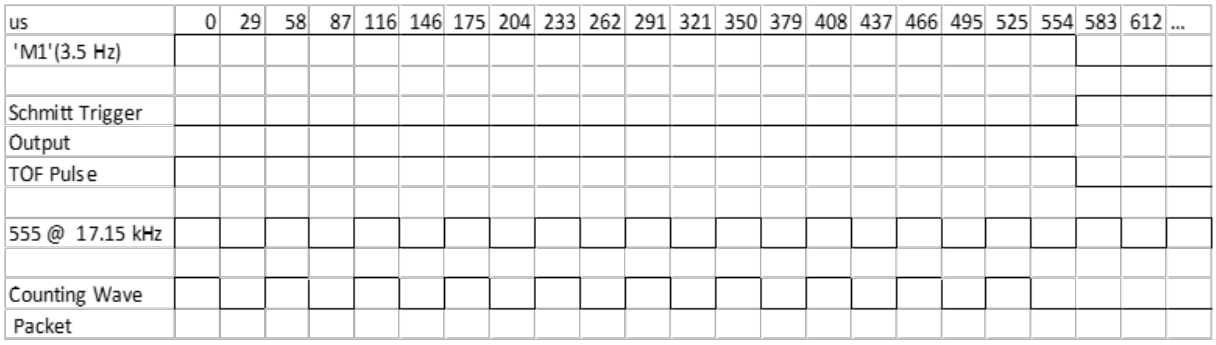

Figure 3: Device Timing Diagram - Minimum Distance Case

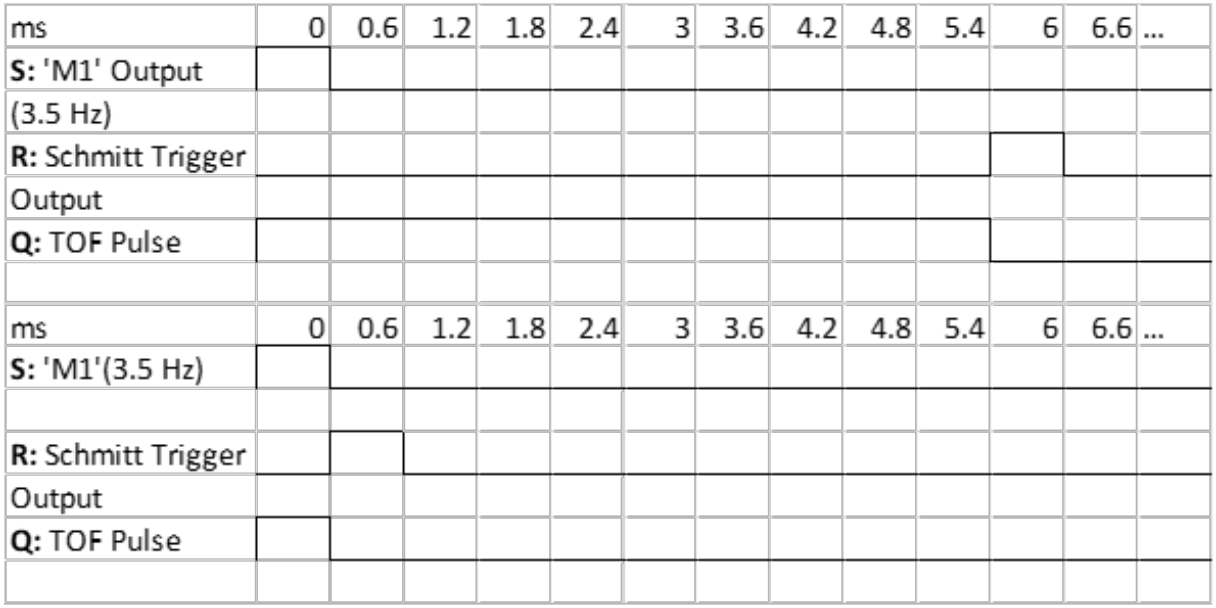

Figure 4: Device Timing Diagram - Maximum Distance Case

The specific components and configurations that were utilized to construct the device are described in detail below.

4.1 Wave Packet Generation

In this section, the method by which an appropriate wave packet was generated is described.

4.1.1 555 Timer 1

In order to drive the piezoelectric material of the transducer at the appropriate driving frequency [4], an astable multivibrator was constructed using the $TLC555$ timer integrated circuit. This timer was constructed such that it would output a 40 kHz square wave with a duty cycle of $\approx 50\%$, since the

piezoelectric transducer data-sheet requires that the transducer be driven at $40 \pm 1\ kHz$ [4]. In order to determine the appropriate external components, equation (4) was used to determine the output frequency of the 555 timer, and equation (5) was used to determine the duty cycle of the timer. In order to precisely control the frequency of this 555 timer, R_b was replaced with a potentiometer for fine tuning. Fine adjustment was necessary in order to drive the piezoelectric transducer is the most efficient manner, maximizing the amplitude of the transmitted sound wave [4]. A complete circuit diagram of 555 Timer 1 is shown below in figure (5).

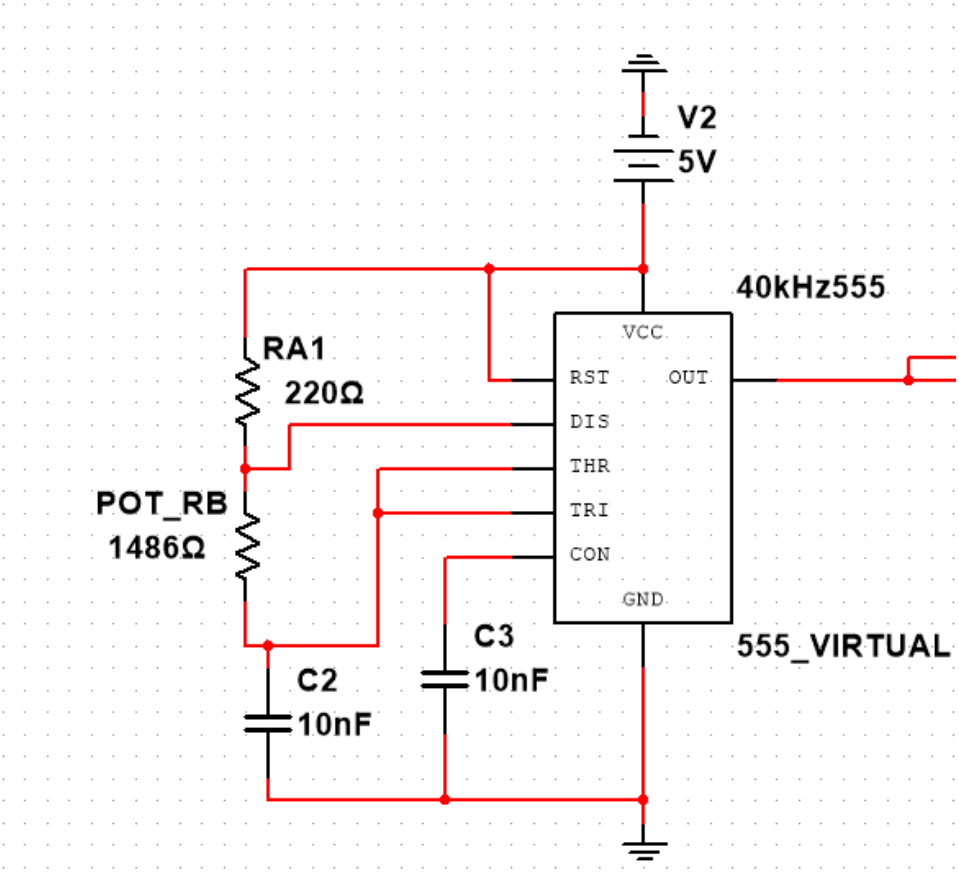

Figure 5: 555 Timer 1: 40 kHz

4.1.2 555 Timer 2

As will be discussed later in section (4.3.1) of this report, in order to receive and process reflection information unambiguously, the 40 kHz driving signal required modulation. Modulation of the 40 kHz signal with a lower frequency resulted in a wave packet, effectively driving the transducer for short periods of time. A graphical example of this concept is included below.

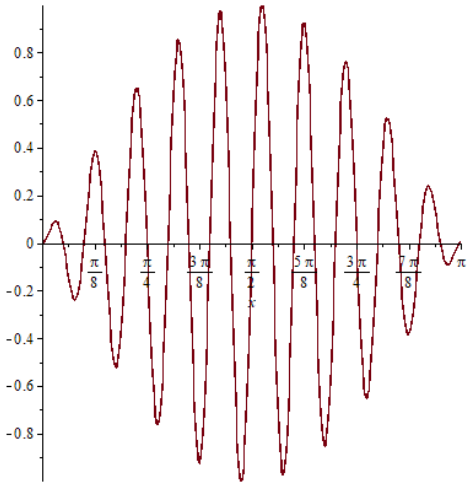

Figure 6: Sinusoidal Wave Packet - General

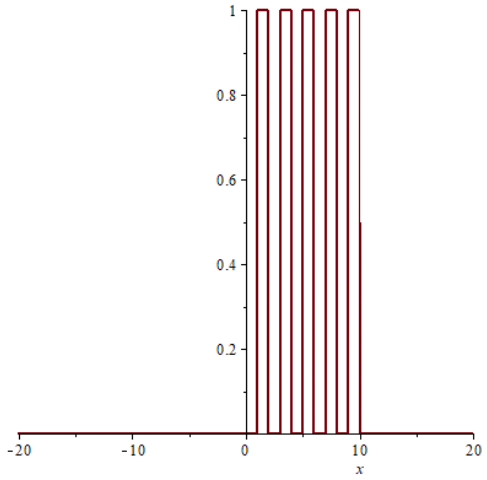

Figure 7: Digitized Wave Packet - Utilized

Thus, 555 Timer 2 was meant to provide a low-frequency packet that served to modulate the high-frequency transducer driving signal (discussed briefly in section (4.1.3)). In order to determine appropriate values for the RC network, there were two important scenarios to consider. First, the minimum distance case was considered. It was required that the Range Finder have the ability to accurately detect distances at a minimum of 10 cm. This corresponds to a time of flight of $\approx 583\mu s$ (see calculation (7) in the appendix). Based on the latching mechanism utilized to generator a time-of-flight pulse (see section (4.3.1)), it was required that the transmitted and received pulse did not overlap in time. Thus, the result of calculation (7) serves as an upper limit for the pulse width of the wave packet. The pulse width of the packet is controlled by the pulse width of 555 Timer 2, thus the duty cycle was tuned in order to lower the pulse width below the maximum. It was much more practical to build a 555 timer with an extremely high duty cycle as opposed to an extremely low duty cycle. Therefore, a device with a high duty cycle was constructed and the output was inverted. In order to generate the desired pulse width the duty cycle was maximized such that the following condition was satisfied.

$$dc_{high} \times T < 580\mu s \tag{1}$$

Where T is the period of 555 Timer 2 and dc_{high} is the percentage of the period for which the output signal is high after inversion. This condition was necessary in order to ensure that the transmitted and received wave packet did not overlap in time at the minimum distance condition. According to equation (5), the duty cycle of 555 Timer 2 was maximized by maximizing R_a, and the resistors utilized yield a duty cycle (% high) of 99.78681%. Once this signal is inverted, the effective duty cycle (% high) was 0.21318%. Thus, the time that the modulation pulse is high is given by equation (9), and is calculated to be $\approx 326\ \mu s$. This pulse width is lower than the maximum stated earlier. In the minimum distance case, the transmitted and received pulses will not overlap in time. The other important case to consider is with regard to the maximum flight distance. The range finder must be capable of accurately determining the distance to the object of interest at a maximum of 99 cm. As a consequence of this requirement, the period at which the slow modulation wave packet is transmitted must be larger than the corresponding maximum time of flight for the ranger finder at 99 cm. In other words, the reflected sound wave pulse must be received before the next pulse is transmitted in order to generate an accurate time-of-flight pulse. Equation (8) was used to calculate the maximum time-of-flight for the device. The maximum time-of-flight was determined to be 5.77 ms. Based on the RC network chosen to satisfy the maximum duty cycle requirements as stated above, the period (see equation (10)) is ≈ 152 ms. It can be seen that the period of the slow modulation wave is larger than the required minimum in order to measure distance accurately at a distance of 99 cm. In conclusion, the RC network that defined the behaviour of the slow modulation wave generated by 555 Timer 2 was determined by ensuring that both extreme

cases outlined above were accounted for properly. A circuit diagram that illustrates the exact values of components utilized to build 555 Timer 2 is displayed below in figure (8).

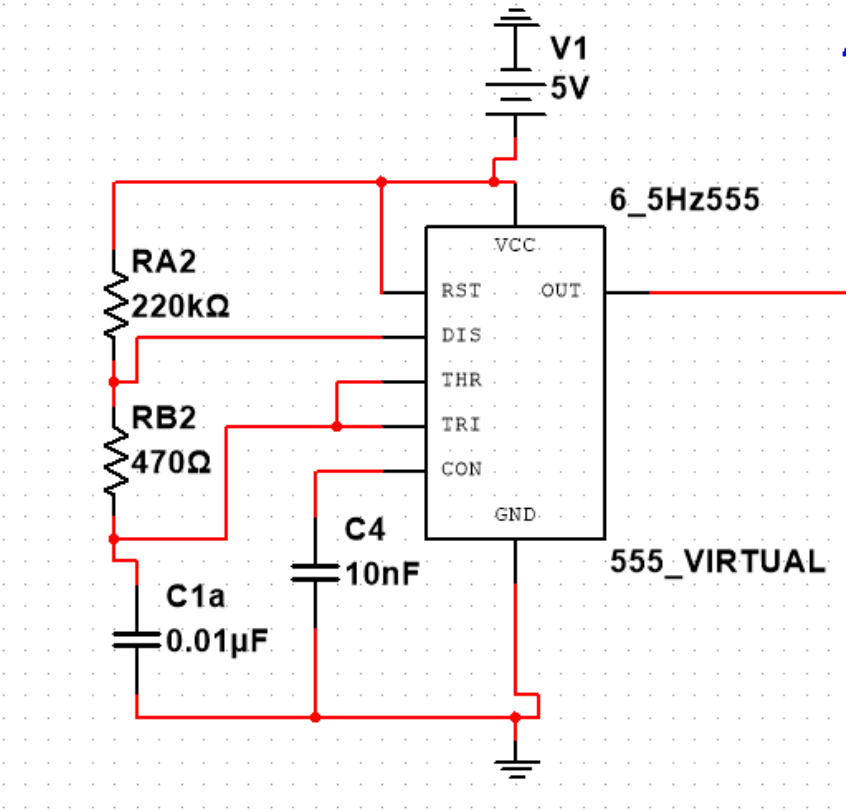

Figure 8: 555 Timer 2: 3.5 Hz

4.1.3 Packet Combination

In order to create the desired wave packet capable of driving the piezoelectric transducer with the desired properties, an AND (SN74HC08N) gate and an inverter (SN74HC14N) were utilized. This combination of logic gates produced the desired pulse shape. A graphical example of this logic circuit is shown below in figure (9). Note that the logic gates utilized in the simulation below are slightly different models than the available physical models.

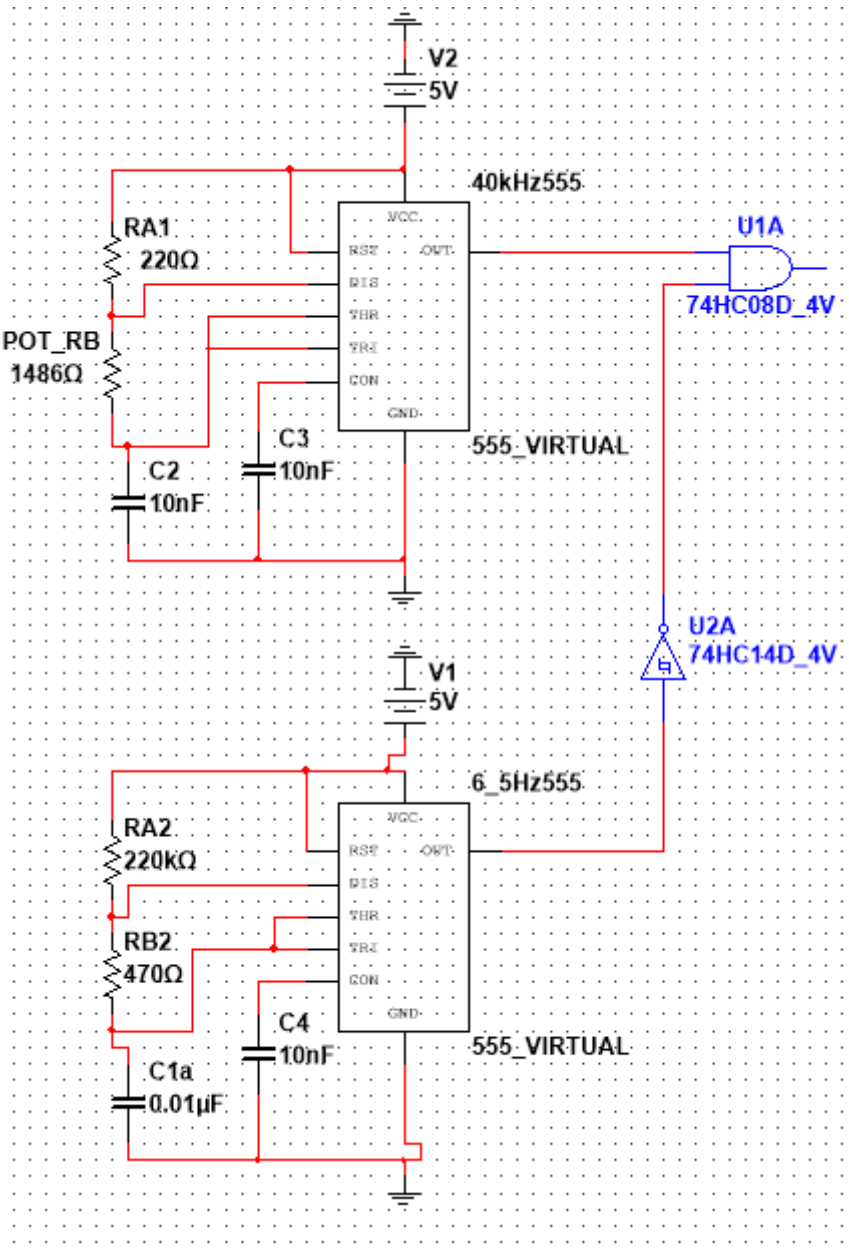

Figure 9: Transmit Packet Combination

4.2 Pre-Amplification, Post-Amplification & Digitization

4.2.1 Pre-Amplification Stage 1

In order to ensure that the sound wave generated by the piezoelectric transducers was of large enough amplitude to survive various attenuation mechanisms at the farthest required distance, a pre-amplifier stage was introduced. The purpose of pre-amplification stage 1 was to increase the amplitude of the voltage signal driving the piezoelectric transducer. A larger amplitude driving signal has the effect of producing larger amplitude sound waves, which in turn are more resistant to attenuation during propagation and reflection. This is desirable because it increases the signal-to-noise ratio in the limiting maximum-distance measurement case and decreases the complexity of the post-amplification and filtering

circuitry that process the received signal. The circuit diagram for the pre-amplification stage is shown below in figure (10). Since only one positive voltage power sources were available, a virtual ground was created with a voltage divider at the non-inverting input of this amplifier. Since the input signal was on the order of 5 V (output from a series of combinational logic gates that is discussed later), a gain of ≈ 2 was chosen. A gain of 2 amplifies the signal up to the maximum possible voltage. The resistor ($R_F 2$) between the output of the pre-amplification stage and the driving input of the transducer was placed in order to limit saturation of the pre-amplification stage operational amplifier. Since the transducer acts as a capacitor when it is driven, the resistor allows for discharge and prevents saturation of the pre-amplification stage.

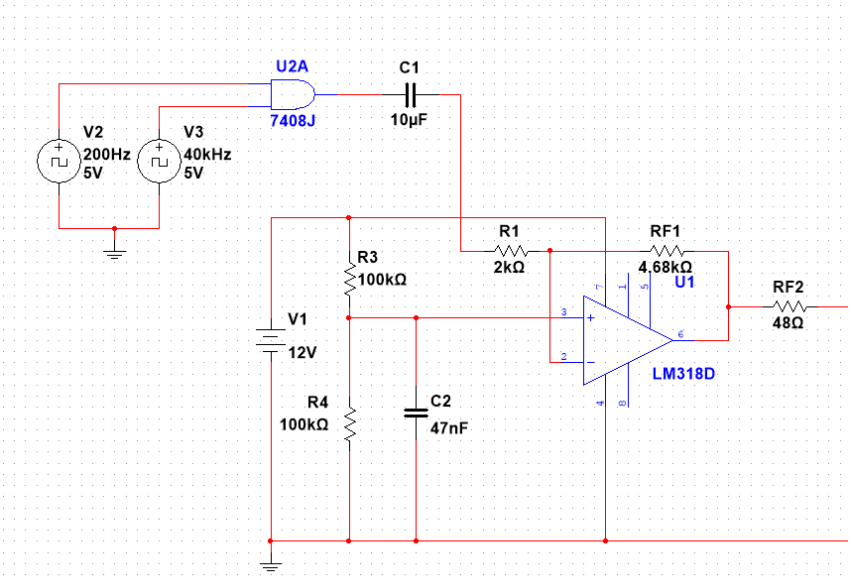

Figure 10: Pre-Amplification Stage

4.2.2 Filter 1 - High Pass

By the method of trial-and-error and viewing the received signal on an oscilloscope, a blocking capacitor was placed in series with the received signal and the input to the first post-amplification stage. A 68 nF capacitor was utilized for this purpose. A circuit diagram of this filter is shown in figure (11). Note that $TRANSOUT$ is the output of the transducer receive pin, and $POA1+$ is the non-inverting input of the first post-amplification stage.

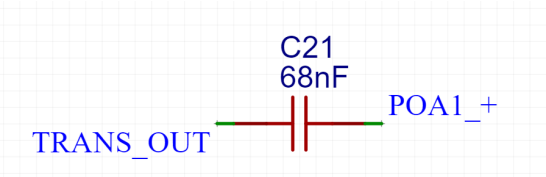

Figure 11: Filter 1

4.2.3 Post-Amplification Stage 1

In order to increase the sensitivity of the device, it was determined that the received signal must be amplified. The qualitatively observed signal to noise ratio of the received transducer signal was lower than desired at far detection distance. Thus, a post-amplifier stage was utilized to amplify the received signal

and increase the device's sensitivity to distance. A non-inverting amplifier was utilized for this purpose. A non-inverting amplifier was used because changing the phase of the input signal would misrepresent the time at which the reflected signal was received. Thus, changing the phase of the received signal during the post-amplification stages would negatively impact the accuracy of the device. If an inverting amplifier were used, a π-phase shift would correspond to an introduced timing error of $\approx 12.5\mu s$ at 40 kHz. According to equation (6), this time difference corresponds to the introduction of an error of 0.428 cm. This error is appreciable as the device is required to accurately measure distance within 1 cm, and thus the non-inverting amplifier was used to avoid this error. The LM318-D operational amplifier was used to create the first post-amplification stage. The circuit diagram can be seen below in figure (12).

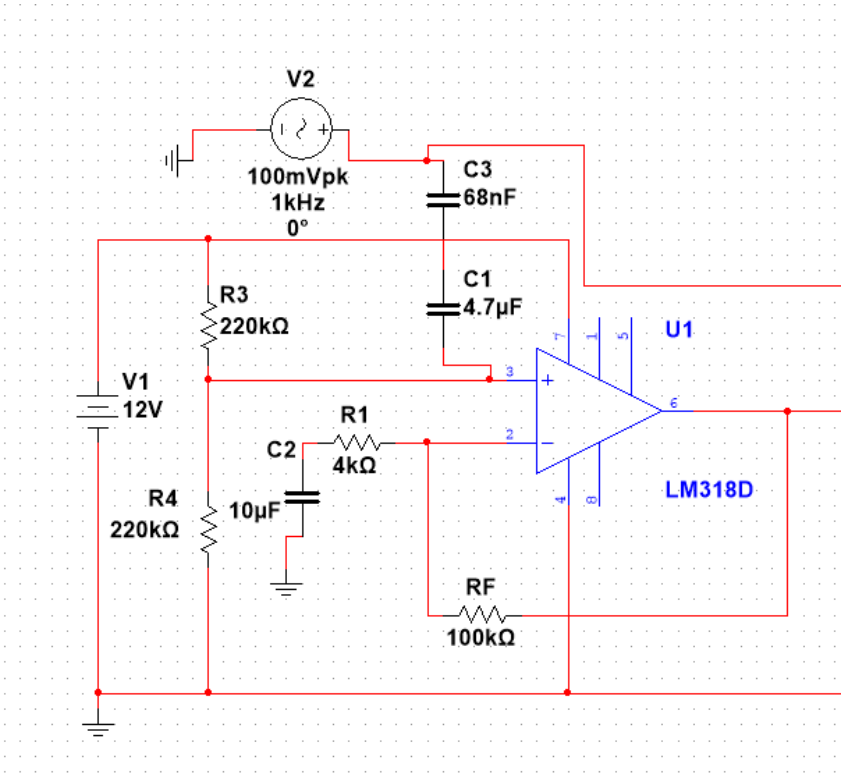

Figure 12: Post-Amplification Stage 1

4.2.4 Filter 2 - Low Pass

Upon inspection of the signal from the first post-amplification stage, it was determined that there was undesirable amplification of noise outputted from the first post-amplification stage. However, the gain of the first post-amplification stage was required in order to sufficiently detect the received signal at the maximum required distance (99 cm). In order to decrease the effect of noise on the post-amplification chain, the gain of post-amplification stage 1 was reduced. Accordingly, another amplification stage was coupled to post-amplification stage 1 which is described in detail in section (4.2.5). The other method used to inhibit amplification of noise was a low pass filter placed between post-amplification stages 1 & 2. Upon inspection of the amplified noise from the output of post-amplification stage 1, an appropriate cutoff frequency was determined to be around 70 kHz. Thus, the filter was designed to pass frequencies below this frequency and attenuate frequencies above this frequency. An appropriate RC network was chosen to satisfy this equation using equation (11) such that $f \approx 70\ kHz$. The low pass filter is displayed below in figure (13).

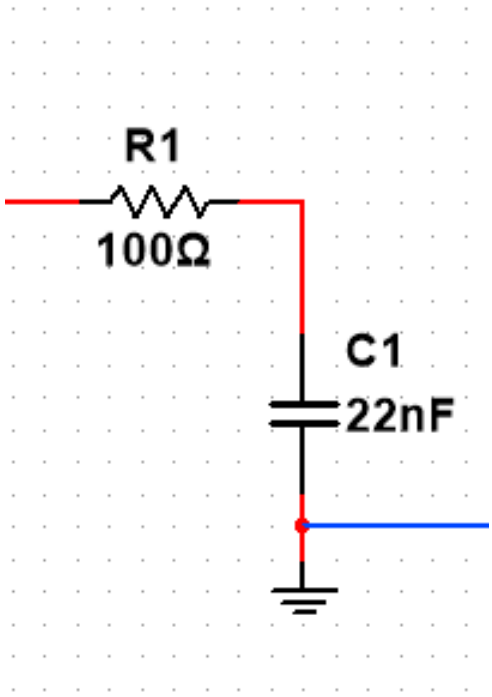

Figure 13: Filter 2 - Low Pass

4.2.5 Post-Amplification Stage 2

As mentioned previously, the gain of post amplification stage 1 was reduced in order to reduce the amplification of noise from the received transducer signal. In addition, a low pass filter was placed between post-amplification stages 1 & 2. Post-amplification stage 2 compensates for the lowered gain regarding post-amplification stage 1. Upon inspection of the received signal at the maximum distance, it was determined that a second amplification stage was necessary in order to sufficiently amplify the signal at the maximum distance. Post-amplification stage 2 was also constructed as a non-inverting amplifier for the same reasons delineated in section (4.2.3). Similar values were chosen for the resistor and capacitor values used to construct this amplifier. The most significant difference between post-amplification stage 1 and post-amplification stage 2 is the gain. The gain is 10× smaller for post-amplification stage 2. It was found that this gain was sufficient to amplify the received signal up to the maximum voltage. Thus, increasing the gain of the amplifier above this value would have no benefit, and would only clip the signal. Post-amplification stage 2 is shown below in figure (14).

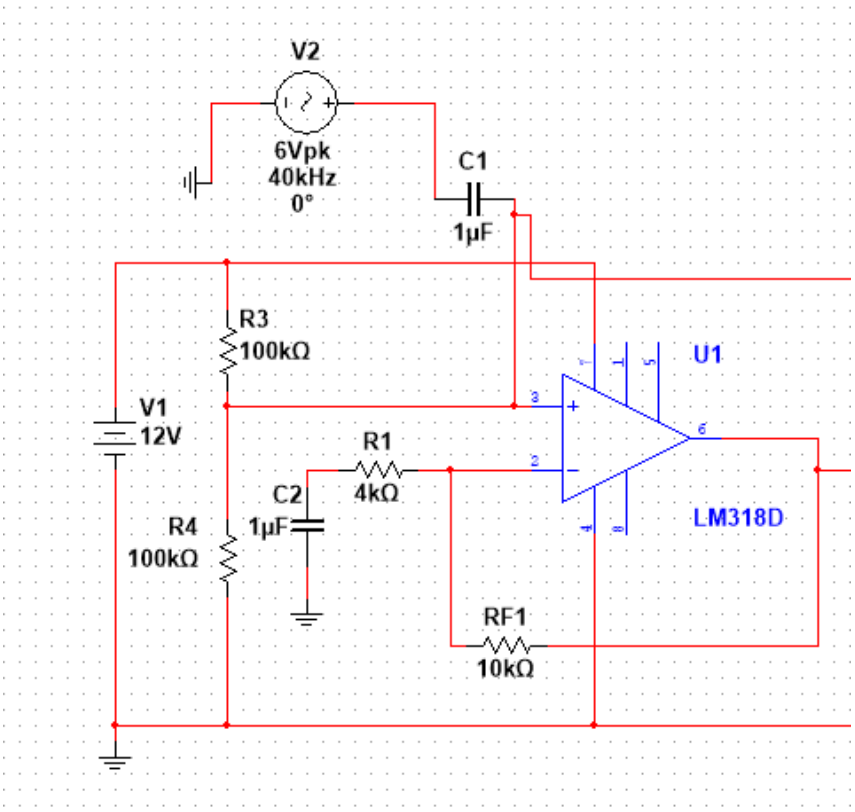

Figure 14: Post-Amplification Stage 2

4.2.6 Schmitt Trigger

At this point in the receive chain, there was an amplified, relatively noise-free 40 kHz signal generated by the reflected sound wave. In order to use this signal as the input to a latch, the signal must be digitized. This digitization was performed using the LM311 comparator, functioning as a Schmitt trigger. Since the amplitude of the amplified signal ranged from $100 - 200\ mV$ to $12\ V$, a significant offset voltage was applied to shift the upper and lower trigger thresholds higher. The upper trigger threshold and the lower trigger threshold were calculated using equations (12) & (13), respectively. The circuit was determined by modifying an example application of the LM311 as a Schmitt Trigger, found in the LM311 datasheet [7]. The resistors and offset voltage were adjusted for this particular application. A circuit diagram of the operational Schmitt trigger is shown below in figure (15). In this diagram, R_3 was included as a potentiometer to retain precise control over the triggering voltage and manually adjust the upper and lower triggering voltages as deemed necessary upon inspecting the signal with an oscilloscope.

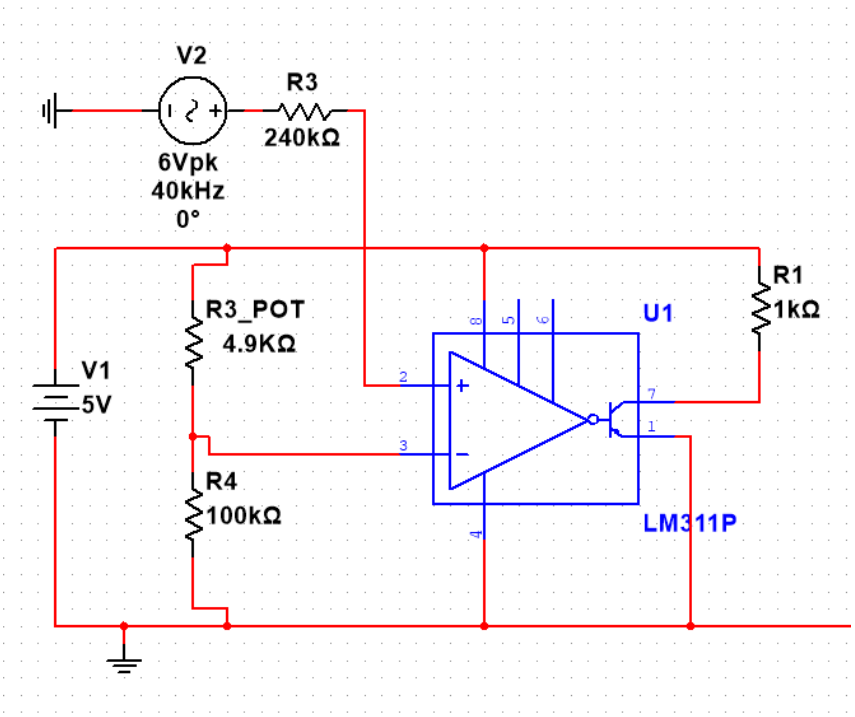

Figure 15: Schmitt Trigger - LM311

4.3 Counting and Display

4.3.1 Latching

In order to generate a digital pulse that represents the time-of-flight of the received sound wave, an SR latch (CD4043BE NOR Latch) was utilized. The truth table for the CD4043BE is shown below in figure (16).

CD4043B

S	R	E	Q
X	X	0	OC*
0	0	1	NC+
1	0	1	1
0	1	1	0
1	1	1	Δ

*OPEN CIRCUIT
+ NO CHANGE
Δ DOMINATED BY S=1 INPUT

CD4043B

Figure 16: CD4043BE Truth Table [8]

The SR latch was connected such that the slow modulation wave was connected to the S input, and the Schmitt-Triggered output is connected to the R input. Initially, both inputs are low, and the output of the latch is low. When the pulse is transmitted initially, the output of the latch gets set high. Once the transmit pulse goes low again, the latch is now in the *latch* state, so the output is still high. When the leading edge of the digitized receive signal is received at the R input, the output of the latch goes low again. This is only true if the transmitted and received pulse do not overlap in time, otherwise the latch enters an undefined state and cannot reliably produce a time-of-flight pulse. This is why the duty cycle of the slow modulation timer (Timer 2) was analyzed and tuned in section (4.1.2). When the digitized 40 kHz square wave now oscillates between 0 and 1, the output will stay low according to the truth table displayed in figure (16). The timing diagram for this configuration can be seen in figure (4). The NOR latch was chosen because it had the appropriate *latch* state, such that the output was held constant when both inputs were low. A circuit diagram of the SR latch is included below in figure (17). Note that the utilized SR latch was not available in Multisim, so the truth table displayed in figure (16) does not apply to the latch in figure (17), although the operating concept described above is still applicable.

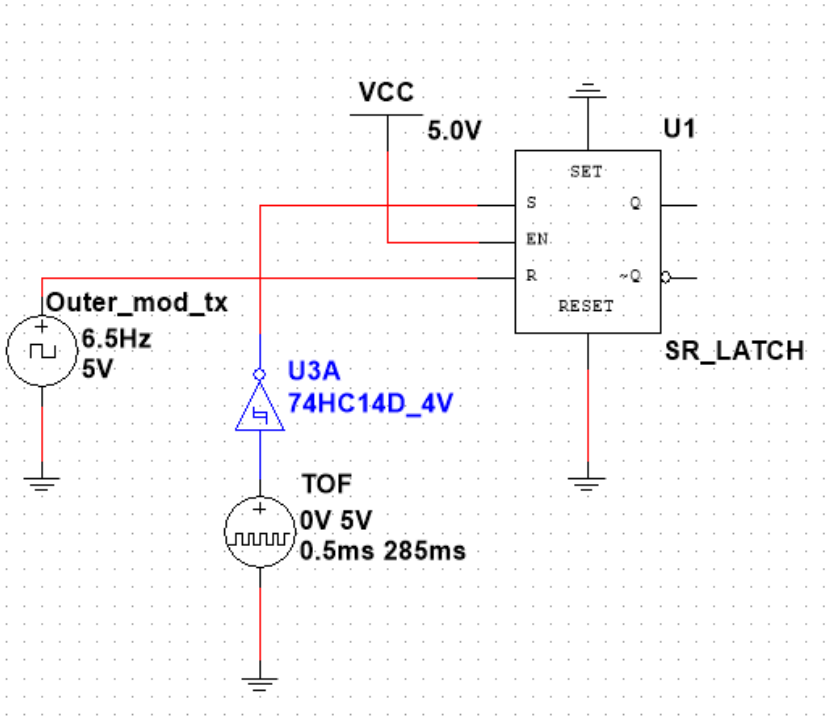

Figure 17: SR Latch Circuit

4.3.2 Counting Timer

At this point in the circuit, a digital time-of-flight pulse has been generated. Now, this pulse must be converted into a distance. In order to convert the time-of-flight signal into a distance, a counter was utilized to increment while the time-of-flight pulse was high. In order to accurately count the number of centimeters represented by this pulse, the correct clocking frequency must be determined. Since the desired resolution of the range finder device is ± 1 cm, each clock cycle will represent 1 cm travelled by the sound wave. The speed of sound can be represented by the following equation, where f is a frequency.

$$v_{sound} = 1\ cm \times f$$
$$f = 34300\ s^{-1}$$

Thus, in order to count one centimeter per clock cycle, the counter circuit should be driven at 34.3 kHz.

However, it is important to recognize that the time-of-flight pulse represents the time-of-flight for the transmitted *and* the reflected sound wave. Thus, in order to determine the distance to the object of interest, the determined distance should be divided by two. A simple way to achieve this result is to count at half of the appropriate frequency that was determined earlier. Therefore, in order to convert the time-of-flight signal into a distance, the counting circuit should be driven at 17.15 kHz. Thus, the desired frequency was achieved by utilizing equation (4) to determine an appropriate RC network. Once appropriate resistor & capacitor values were chosen, the resistors were changed slightly to adjust the duty cycle towards 50%. Note that the duty cycle was calculated using equation (5). A circuit diagram of 555 Timer 3 that includes the specific RC network utilized is included below in figure (18). Note that the resistor R_1 in figure (18) is a potentiometer, which is adjustable in order to tune the frequency of 555 Timer 3 precisely on the board.

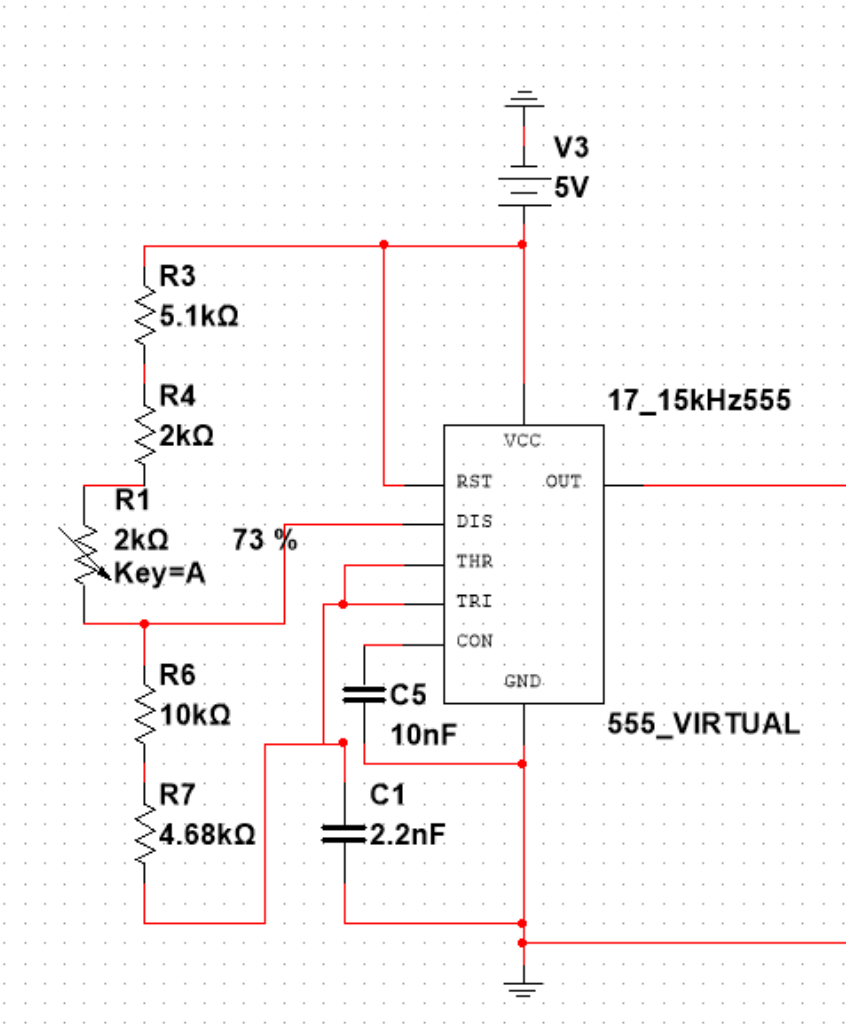

Figure 18: 555 Timer 3 - 17.15 kHz

4.3.3 Counting

The reasoning that justifies setting the clock frequency as 17.15 kHz for the clock signal used to drive the counter circuit has been discussed above in section (4.3.2). To generate a wave packet for appropriate counting, the time-of-flight pulse and the counting 555 Timer were passed through an AND gate

(SN74HC08N). In order to count up to a maximum of 99 cm, two 4-bit asynchronous ripple counters were constructed using two CD4510B BCD counters. In theory, only 7 bits are needed as the maximum decimal representation of a 7-bit binary number is 128. A 6-bit binary value would not suffice. Equation (14) was used to determine the maximum equivalent decimal number that can be represented using n bits. However, the CD4510B counters are only supplied in multiples of 4 bits. In this use case, each digit (the $10s$ digit and the $1s$ digit) was represented as an individual 4-bit binary number. In order to configure a series of CD4510B counters as an asynchronous ripple counter, an example circuit was utilized - this circuit is shown in the CD4510B datasheet [9]. This circuit is also shown below in figure (19). There are pulse voltages that represent the slow modulation wave and the digitized, received signal. Note that the outputs of the counter are labelled according to which position they represent in each 4-bit binary number that accordingly represents each digit. In the diagram below, bits labelled T represents the $10s$ digit, while bits labelled O represent the $1s$ digit. Note that in each case, the LSB is labelled 1 and the MSB is labelled 4.

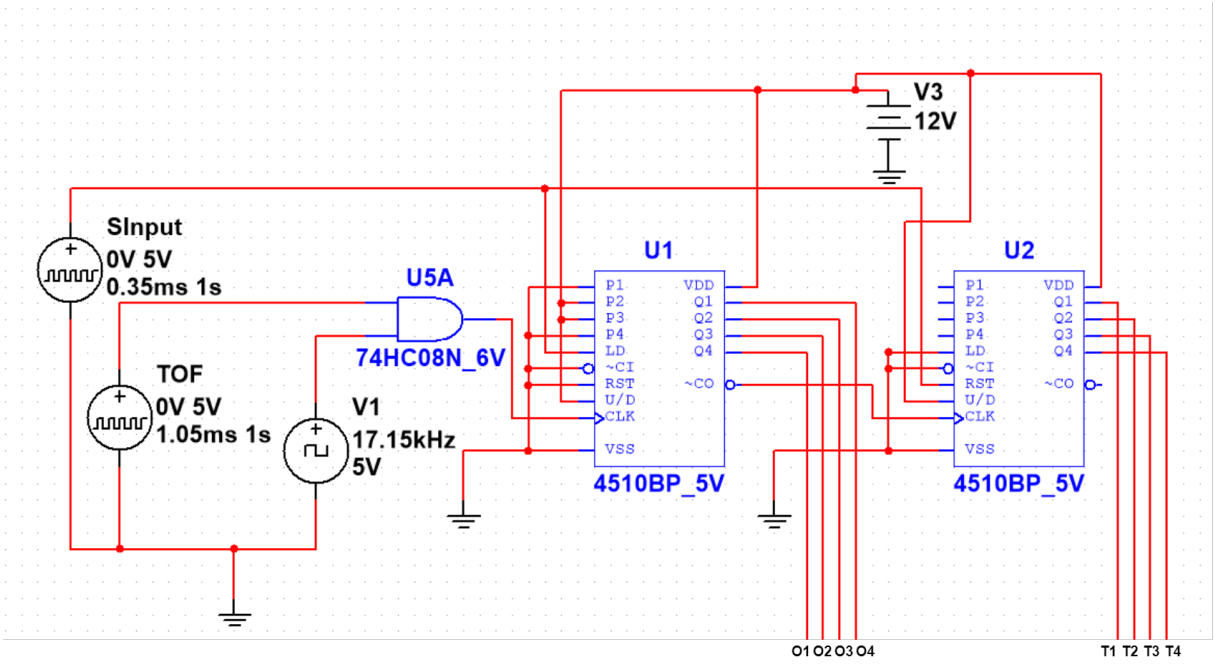

Figure 19: Counter Circuit

4.3.4 Display

Finally, the last module of the device was the display module. This module consists of two CD74HC4511E decoders, and two 24AJ1494 display modules. The decoders were fed by the appropriate binary outputs from each counter mentioned in the previous section. In addition, there were 220Ω current-limiting resistors placed in series with the decoder outputs in order to limit the current through each LED segment in the 24AJ1494 display modules. Note that the labels describing these resistors are obscured in the figure below (20), yet they are all 220Ω. A circuit diagram of this module of the device is shown below in figure (20).

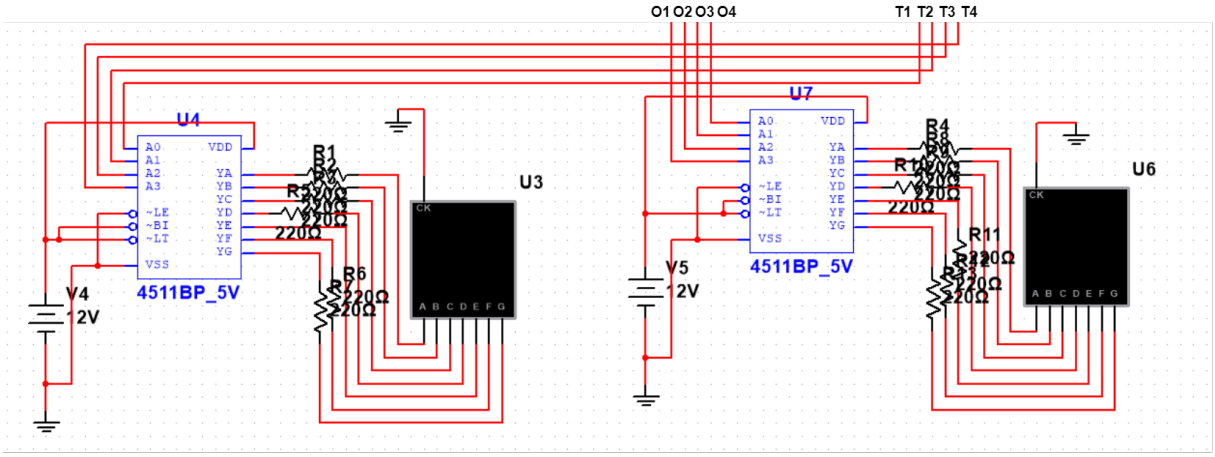

Figure 20: Decoder & Display Circuit

5 Results

5.1 Final Product

The final Ultrasonic Range Finder can be understood appropriately by subdividing the device into two working modules; an analog processing module and a digital processing module. The purpose of the analog stage of the device is to produce an appropriate driving signal for the piezoelectric transducer, and process the received signal such that it is suitable for the digital stage of the device. The purpose of the digital stage of the device is to convert the received analog signal into a distance, and display the result of this conversion to the user in a meaningful fashion. The specific sub-modules that were used to construct the analog & digital stages of the device were discussed in more detail in section (4). A circuit diagram that contains each independent module connected together is shown below in figure (21).

5.2 My Work

In developing and constructing this device, responsibility for each module was allocated equally between group members. During this project, others constructed the digital portion of the device, while I worked on the analog portion of the device. Eventually, multiple group members constructed the entire device (both the analog and digital stages). However, the design process was allocated to different group members. I personally constructed the analog stage of the device. I created the transmission wave packet which consisted of two 555 Timers (1 & 2). Next, transmission wave packet was amplified before transmission via Pre-Amplification Stage 1. Then, the Post-Amplification chain was constructed. This chain included Filter 1, Filter 2, Post-Amplification Stage 1 & Post-Amplification Stage 2. Each amplifier in the post-amplification chain was constructed independently and tested before the modules were connected together to create the final product. There was one change made that deviates from the circuit diagrams shown above in section (4). This modification was necessary in order to ensure that our device was functional. Based on probing the system with the handheld Oscilloscope (Hantek2000), the result of combining the signals from 555 Timer 1 & 555 Timer 2 did not behave as expected. The AND gate should have produced a wave packet at 40 kHz for a short period of time (governed by 555 Timer 2), and a digital LOW signal otherwise. It was observed that there was a small amplitude 40 kHz square wave signal produced at the output of the packet combination during the LOW period of the signal. This was a problem because the wave packet was amplified before driving the piezoelectric transducer. Thus, the undesired small-amplitude signal was amplified. As a consequence, it was difficult to perceive discrete received signal packets after both post-amplification stages. Extra Schmitt-triggered inverters (SN74HC14N) were available on the board, so the wave packet was passed through an inverter twice before

amplification. The undesirable small-amplitude 40 kHz signal could not be filtered with a frequency-sensitive method as it was at the same frequency as the desired high-voltage wave packet. Thus, it was removed from the transmission signal by an amplitude-sensitive method. The Schmitt triggers in the inverters effectively removed the undesired small-amplitude signal before amplification. Following this change, discrete sinusoidal wave packets were observed at the output of the post-amplification chain.

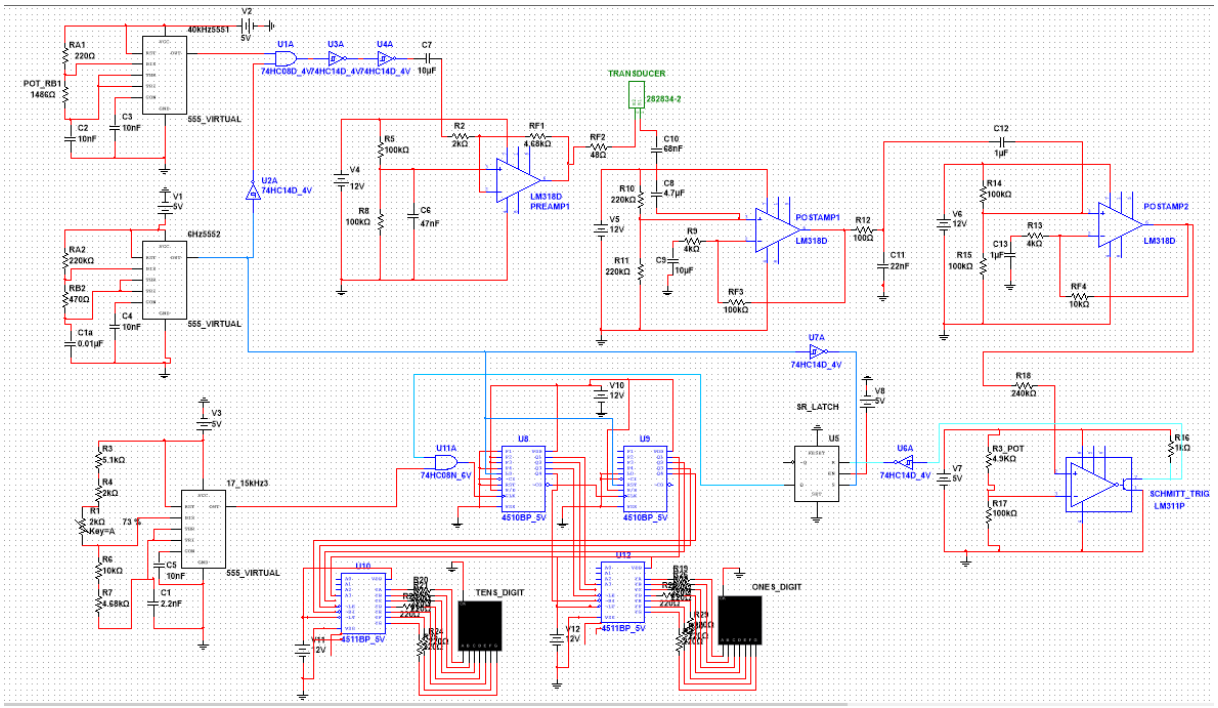

Figure 21: Complete Circuit Diagram

5.3 Testing & Measurement

In order to test the device, the range finder was placed on a long flat bench alongside a measuring tape. At first, it was found that the range finder reported a distance that was larger than the measured distance by about 10 cm. Most likely, this is due to the fact that the speed of sound was not exactly $34300 \frac{cm}{s}$. The speed of sound was likely smaller than the assumed value when these measurements were made. The speed of sound generally increases as the density of the medium through which sound propagates decreases [6]. There are two effects of interest that effect that speed of sound; namely the temperature & humidity. The humidity of an environment effects the speed of sound because water molecules have less mass than typical air molecules (such as Nitrogen, Oxygen and Carbon Dioxide). When a greater percentage of the propagation medium (air) is made up of water molecules, the density is effectively decreased. So an increase in humidity would lead to a lower density medium and faster propagation of sound. However, the effect of humidity on the speed of sound propagation is usually second-order compared to other effects [6]. As the temperature of the medium changes, so does the density of the medium. In this way, temperature effects the speed of sound through the general relation: $v_{sound} \propto T$. We observed that the device consistently produced distance readings that were too high. Based on the environmental conditions in which the test was performed, this means that the speed of sound was slower than expected. In order to tune the device, we decreased the frequency of the 555 timer driving the digital counting circuit to account for the fact that the speed of sound was slower than expected. A variable resistor was placed in the RC network that allowed the frequency of the counting timer to be adjusted. When the frequency was sufficiently lowered, the accuracy of the distance output improved.

Once the counting frequency was tuned to produce a reasonable output, a set of distance measurements were taken such that the same measurement was repeated multiple times at a single distance. Then, the standard deviation of the data was calculated at each distance at which the measurement was repeated multiple times. The equation used to calculate standard deviation is shown in the appendix (3). The frequency of the counting timer at which this data was taken was recorded using the *Hantek2000*. The second set of data was taken after the frequency of the counting timer was increased in an effort to increase the accuracy of the device. Again, the frequency was measured using the *Hantek2000*. Note that the uncertainty in the measured frequency comes from the *Hantek2000* datasheet [10]. Both sets of data are included below in figure (22). In addition, the ideal mapping such that the measured distance corresponds exactly to the displayed distance is shown on the plot for reference. Note that each data point displayed on the chart is an average of 5 measurements taken at the same distance. The uncertainty in each data point is quantified using equation (3) and displayed as an error bar.

$$f_1 = 15.10 \pm 0.1\%\ kHz$$

$$f_2 = 15.50 \pm 0.1\%\ kHz$$

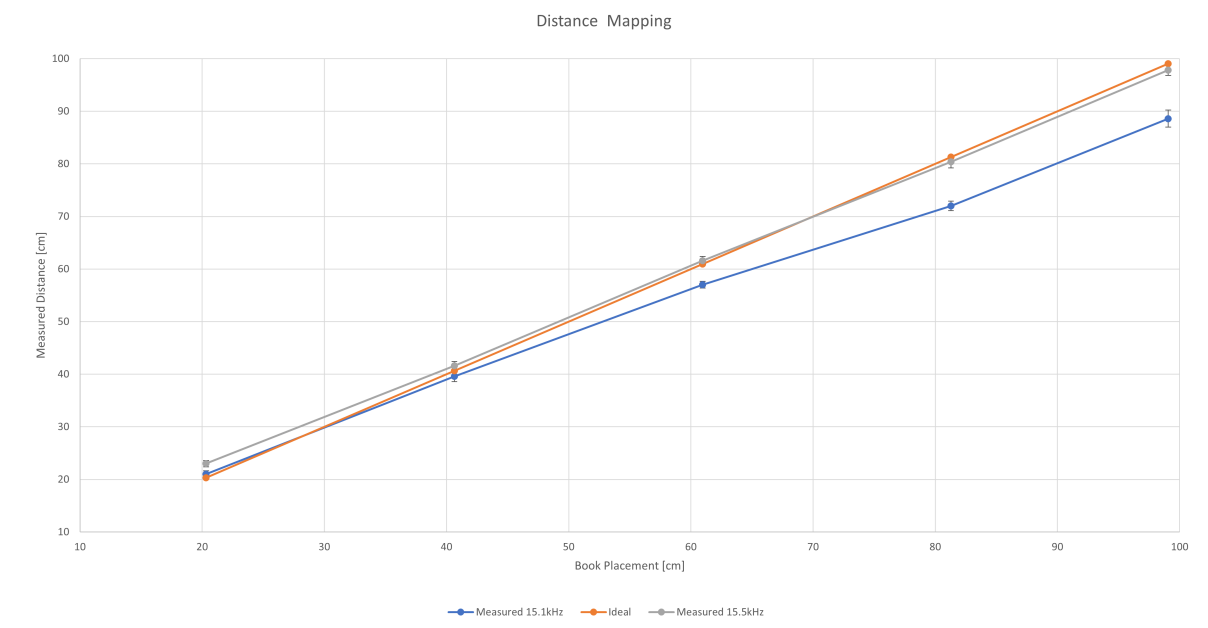

Figure 22: Measured Distance Mapping

Referring to figure (22), it can be seen that the magnitude of the error over most of the measurement interval decreased when f_2 was utilized as the counting frequency. It is apparent that the ideal scenario does not fall within the error bars that represent the error in the measurements made by the device. However, when the correct frequency is employed (f_2), the ideal measurement case falls within the error of the measured distance data at most of the points. The error in the distance measurement performed at smaller distances is higher when compared to the rest of the measurement range.

The Counting Timer (555 Timer 3) has the most significant impact on the accuracy of the device. Therefore, an error analysis of the frequency of the 555 timer will be performed in order to account for variations in the frequency produced by the timer. As a reminder, the Counting Timer circuit is shown below in figure (23).

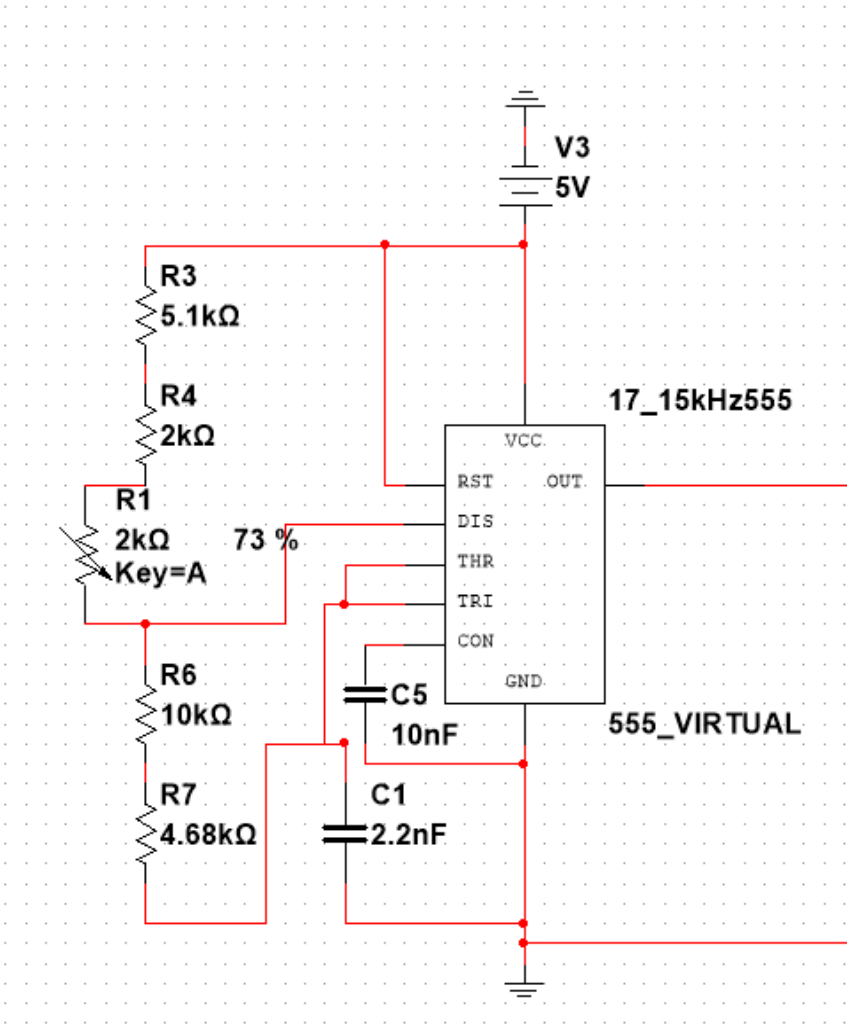

Figure 23: 555 Timer 3 - Counting

The equation that governs the frequency of this 555 timer is given below (2).

$$f_{555} = \frac{1}{((R_1 + R_3 + R_4) + 2(R_6 + R_7)) \times ln(2)C_1} \tag{2}$$

In order to perform an error analysis of the frequency, common error combination formulas are utilized. This process is laid out step-by-step below. It is also noted that the uncertainty on each resistor is given as $\delta R = \pm 1\%$.

Let $R_\alpha = R_1 + R_3 + R_4$ and $R_\beta = R_6 + R_7$.

$\sigma_{R_\alpha} = \sqrt{(\sigma_{R_1})^2 + (\sigma_{R_3})^2 + (\sigma_{R_4})^2} = \pm 56.7\Omega$

$\sigma_{R_\beta} = 2 \times \sqrt{(\sigma_{R_6})^2 + (\sigma_{R_7})^2} = \pm 220.8\Omega$

Note that the uncertainty in the capacitor C_1 is not given. Let γ be defined such that $\gamma = \frac{1}{f}$.

$\sigma_\gamma = ln(2) \times \sqrt{(\sigma_{R_\alpha})^2 + (\sigma_{R_\beta})^2} = 158.01s$ Therefore the uncertainty in the measured frequency of the signal produced by 555 Timer 3 is defined.

$$\sigma_f = 158.01\ s^{-1}$$

The uncertainty quoted by the *Hantek2000* is added in quadrature to the uncertainty calculated above, applied to the more accurate counting frequency (f_2) and is shown below.

$$\sigma_{total} = \sqrt{(\sigma_f)^2 + (f_2 \times 1\%)^2} = \pm 158.76\ s^{-1}$$

The uncertainty quoted above (σ_{total}) corresponds to $\pm 0.5\ cm$ when utilized to determine a distance. Now that the uncertainty in the frequency of 555 Timer 3 has been accounted for, the error bars on the measurements taken using f_2 can be expanded accordingly. An updated plot with the error of 555 Timer 3 accounted for is shown below in figure (24). Note that f_1 data is removed from this plot. It can be seen that the error bars have increased in length. However, data at the close end of the measurement range is still outside of the accepted uncertainty of the device. This suggests that there are other sources of error that could have made minor contributions to inaccuracy in this device.

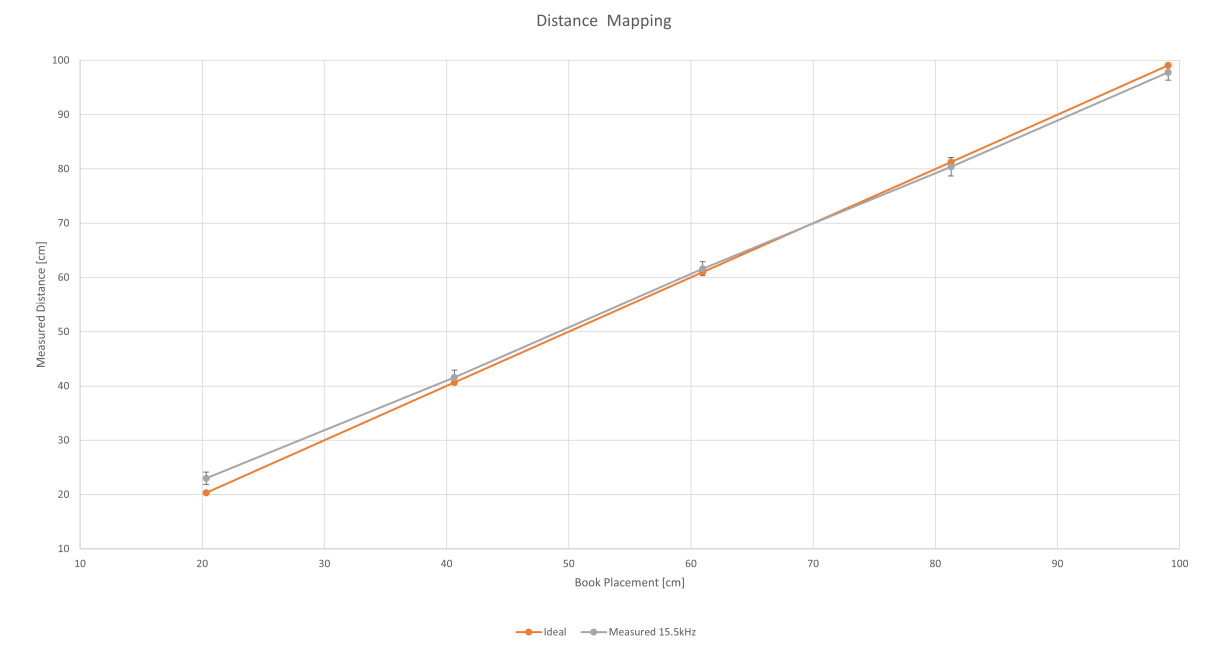

Figure 24: Distance Mapping f_2 - Updated Error

6 Lessons Learned

There were many challenges encountered by the team throughout the duration of this project. Usually, electronic components such as operation amplifiers are studied is isolation. After successfully completing this project, the team now understands the importance of constructing the device as a series of isolated modules. The concept of top-down design was utilized during the early design phase of the project. First, the functional goals of the device were described on a high level. Next, these goals were broken down into sub-goals. Then, thorough consideration was given to the means by which these sub-goals would be achieved. This process naturally led to the description of isolated modules to perform a specific sub-task, such as generating a 40 kHz square wave for example. The next step of the design process that was utilized is referred to as bottom-up synthesis. Each module was constructed by various members of the team in isolation. These modules were also tested in isolation in order to ensure that they behaved as expected. After each module was designed, constructed and tested, the team referred to the high-level diagram created during the top-down design process and connected the appropriate modules. Connecting individual modules successfully was the most challenging part of this design project. It was often the case that the behaviour of a specific module differed slightly when connected to other modules. Small

tweaks had to be made to account for these changes. These problems were the most difficult to solve because the behaviour of a specific module was no longer isolated, but was dependent on the properties of other modules. In particular, impedance matching between amplifier circuits was a challenging task. There was only one major design change implemented during the synthesis stage of the project. Our initial plan was to use a monostable multivibrator to control the transmission packet pulse width. As discussed previously, pulse width control became necessary as a consequence of the latching mechanism utilized to generate a time-of-flight pulse. However, we determined that using a monostable multivibrator to achieve the desired pulse width was not practical. Instead, the duty cycle of the slow modulation timer was pushed towards it's upper limit, and the signal was inverted in order to precisely control the maximum modulation pulse width. Otherwise, the high-level design modules were constructed independently and integrated with success. In conclusion, the team learned that building and verifying modules with a concisely defined sub-goal was an effective method of bottom-up synthesis. Once individual verification was complete, analog and digital system integration could be performed.

7 Conclusion

In conclusion, the team successfully designed and built an Ultrasonic Ranger Finder using the principles of Top-Down design & Bottom-Up Synthesis. The device reported results accurate to within $\pm 2\ cm$ over the entire desired range. A few design modifications were made during construction of the device, and the team adapted to these changes effectively; producing a final working product with the desired accuracy and range.

8 Appendix

$$\sigma = \sqrt{\frac{\sum_{i=1}^{N} (x_i - \mu)^2}{N}} \tag{3}$$

$$f = \frac{1}{(R_a + 2R_b)\, C ln(2)} \tag{4}$$

$$dc_{low} = \frac{R_b}{R_b + R_a} \tag{5}$$

$$\delta x(t) = \frac{34300\ cm}{1\ s} \times t\ s \tag{6}$$

The minimum time of flight was calculated using the inverse of the speed of sound in air [6], and the distance travelled by the sound in the medium. The distance travelled by the sound was the distance to the object of interest, multiplied by a factor of 2 to account for transmission and reflection.

$$TOF_{min} = \frac{1\ s}{34300\ cm} \times 2 \times 10\ cm \tag{7}$$

The maximum time of flight was calculated using the speed of sound in air [6], and the distance travelled by the sound in medium. Again, the distance travelled by the sound was the distance to the object of interest, multiplied by a factor of 2 to account for transmission and reflection.

$$TOF_{max} = \frac{1\ s}{34300\ cm} \times 2 \times 99\ cm \tag{8}$$

$$t_{up} = \frac{dc_{high}}{f} \tag{9}$$

$$f = \frac{1}{T} \tag{10}$$

$$f = \frac{1}{2\pi RC} \tag{11}$$

$$V_{UT} = V_{offset} \times \frac{R_2}{R_1 + R_2} + V_0 \times \frac{R_1}{R_1 + R_2} \tag{12}$$

$$V_{LT} = V_{offset} \times \frac{R_2}{R_1 + R_2} - V_0 \times \frac{R_1}{R_1 + R_2} \tag{13}$$

$$max_{decimal} = 2^n - 1 \tag{14}$$

Just for fun (and practice), a PCB (Printed Circuit Board) was fabricated that represents the range finder system that was built. Some photos are included below for interest.

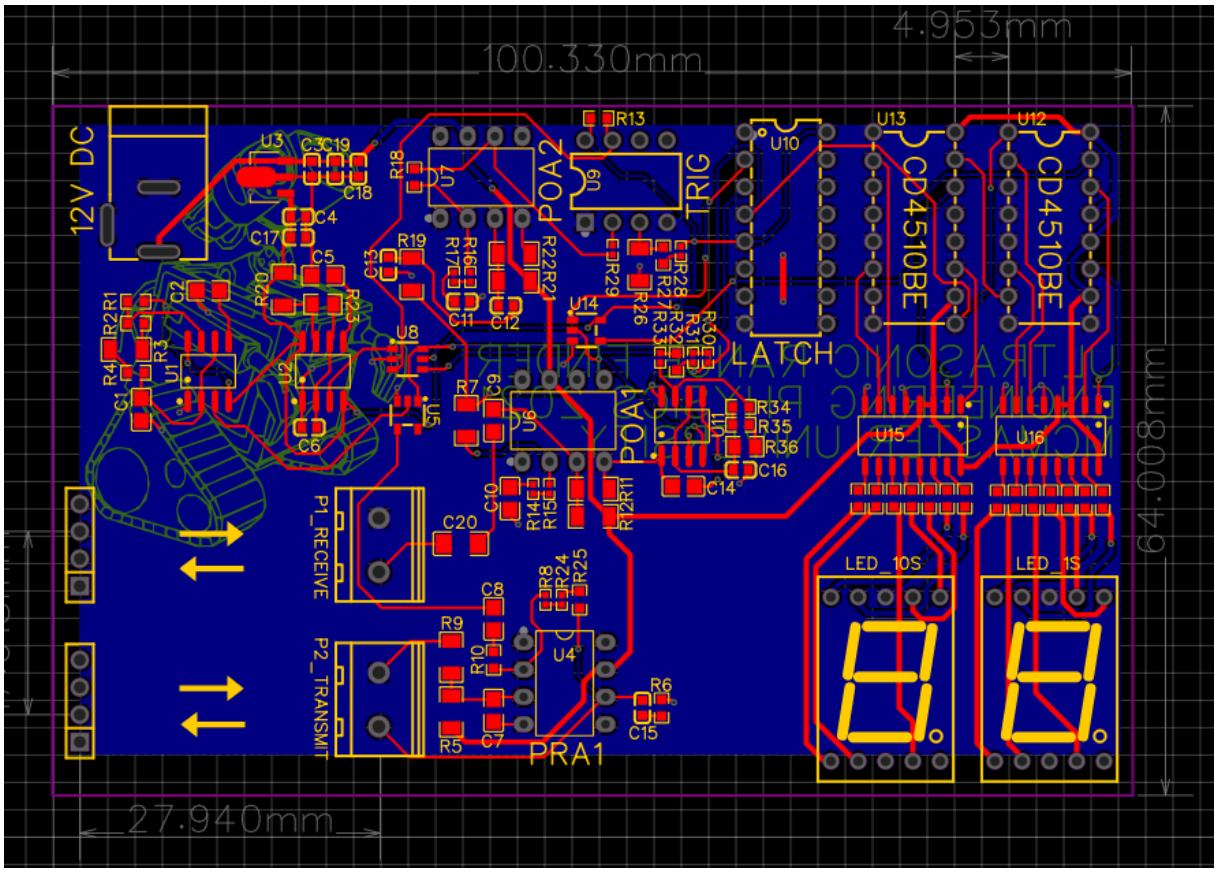

Figure 25: Routed PCB

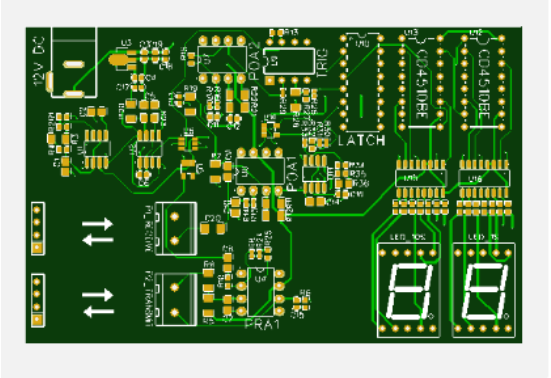

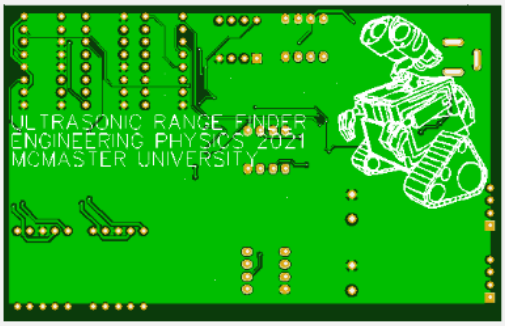

Figure 26: PCB Gerber File(s)

References

[1] C. Rusu, "What is the Piezoelectric Effect?," OnScale, Sep. 16, 2019. https://onscale.com/blog/what-is-the-piezoelectric-effect/ (accessed Nov. 10, 2021).

[2] Admin, "What is The Normal Ultrasound Frequency Range for Humans?," Ox Science, Nov. 21, 2020. https://oxscience.com/ultrasound-frequency-range/ (accessed Nov. 10, 2021).

[3] R. Lunawat, "What Is A Dipole? What Is Dipole Moment?," Science ABC, Jan. 01, 2020. https://www.scienceabc.com/pure-sciences/what-is-a-dipole.html (accessed Nov. 10, 2021).

[4] M. Sensors, Air Ultrasonic Ceramic Transducers. MIDAS Sensors.

[5] Anders Brahme, M. Mischi, N. G. Rognin, and M. A. Averkiou, Comprehensive biomedical physics, vol. 2. Amsterdam Etc.: Elsevier, Amsterdam [Etc, 2014, pp. 361–385.

[6] "Air - Speed of Sound," www.engineeringtoolbox.com. https://www.engineeringtoolbox.com/air-speed-sound-d_603.html#: :text=Speed%20of%20Sound%20in%20Air%20at%20Standard%20Atmospheric (accessed Nov. 25, 2021).

[7] T. Instruments, "LM111, LM211, LM311 Differential Comparators," Texas Instruments Incorporated, Dallas, Texas, Mar. 2017. Accessed: Nov. 19, 2021. [Online].

[8] H. Semiconductor, "CMOS Quad 3-State R/S Latches," Texas Instruments Incorporated, Dallas, Texas, Oct. 2003. Accessed: Nov. 22, 2021. [Online].

[9] H. Semiconductor, "CMOs Presettable up/Down Counters," Texas Instruments Incorporated, Dallas, Texas, Jul. 2003. Accessed: Nov. 21, 2021. [Online].

[10] H. Electronic, Hantek2000 Series Handheld Scopemeter User Manual, vol. V 1.1.